Optimization of Yard Sectional Shape and Configuration for a Modern Clipper Ship

Tyler Doyle[1], tyler@stanford.edu
Margot Gerritsen[2], margot.gerritsen@stanford.edu
Gianluca Iaccarino[3], jops@stanford.edu

Abstract

A computational fluid dynamics (CFD) based optimization procedure is used to study the rig of the modern clipper ship the *Maltese Falcon*. We optimize the sheeting angle and camber of the yards of two-dimensional cross sections of the rig. A gradient-based cost function minimization algorithm and an optimization algorithm based on Evolutionary Strategies (ES) are combined with a RANS CFD model to perform the optimization. Results for optimizing the sheeting angles of 12 percent camber circular sections are presented as well as results for optimizing both the sheeting angle and the camber.

1 Introduction

Sail shape optimization is challenging because of the complex coupling between the aerodynamic forces produced by a sailboat's rig and the hydrodynamic forces produced by its hull and underwater appendages [2]. Yacht designers generally assume a steady-state sailing condition setting rig forces in equilibrium with hull forces for the purpose of estimating performance. This assumption forms the basis of the widely used Velocity Prediction Programs or VPPs. Accurate numerical modeling of the complete boat (sails, hulls and appendices) is extremely expensive from a computational point of view and not practical if many different configurations and flow conditions have to be investigated. In our sail optimization research, we therefore rely on simplified models to handle the hull forces and the interaction between hull and sail forces. We use CFD to accurately compute the flow past the sails and the aerodynamic forces on the rig.

The typical goal of sail shape optimization is to produce a configuration that optimizes the velocity made good (VMG) for a given apparent wind speed and direction. In many respects, a sail resembles an airplane wing and similarly it generates a lifting force, L, perpendicular to the free stream flow, and a drag force, D, in the direction of the free stream flow. At different apparent wind angles the optimal force configuration will be different. The essential requirement of a sail is to generate a large driving force Cx along the centerline of the boat. But, except when sailing dead down wind, this is not possible without producing a heeling force Cy perpendicular to the centerline at the same time. The heeling force must be balanced the stability of the hull and a side force produced by the underwater appendages. The stability of the hull and the efficiency of the underwater appendages therefore put a limit on the driving power that can be extracted from the wind. The relation between lift and drag, and driving and heeling force is determined by the sheeting angle a sail is set at relative to the centerline of the boat. In upwind conditions a sail is set at a small sheeting angle. Most of the lift produced is directed perpendicular to the centerline producing a large heeling force and small driving force. The optimization criterion is therefore generally to maximize the driving force to heeling force ratio. When a boat bears away to a reach, the sheets are eased which results in the lift contributing more to the driving force and less to the heeling force. Because the hull now needs to balance a smaller heeling force, more lift can be tolerated. When sailing on a beam reach most of the force produced by the rig acts along the centerline and thus a high lift coefficient is needed. On downwind courses, the only criterion for sail efficiency is maximum drag of the rig.

---

[1] Doctoral Candidate, Department of Mechanical Engineering, Stanford University
[2] Assistant Professor, Stanford Yacht Research (http://syr.stanford.edu), Stanford University
[3] Research Associate, Center for Turbulence Research, Stanford University

Presently most sail shape optimization is performed using parametric studies where design variables such as camber, draft and twist are adjusted in a trial-and-error fashion to maximize a certain performance measure. The performance of a given sail configuration can be evaluated using full scale testing, wind tunnel testing or numerical simulation (CFD). Full scale testing is of course most accurate but also most expensive and time-consuming. Wind tunnel measurements are also expensive and in addition it is difficult to accurately scale down to the model size. Computational fluid dynamics has the potential to evaluate the performance of a given sail shape accurately, and with a shorter turn-around time. CFD calculations also provide a more detailed description of the flow field than both wind tunnel testing and full scale testing, and can therefore contribute to a better understanding of the optimization problem. CFD techniques have been successfully applied to shape optimization problems in the aerospace industry for a number of years. A major advantage of using CFD to evaluate the forces produced by a sail is that CFD solvers can be easily integrated with optimization procedures to automatically search for optimized sail shapes.

The goal of our current work is to explore the possibility of using automated optimization algorithms coupled to CFD for sail shape optimization. There are two major categories of shape optimization techniques; adjoint and iterative methods. Adjoint methods calculate the optimal shape via the solution of an adjoint problem obtained from the governing equations describing the fluid flow. It is effective because the cost of an adjoint solution is typically equivalent to that of the original problem, and most importantly, independent from the number of design variables [2]. The adjoint method has become a popular choice for design problems involving inviscid fluid flow, and has been successfully used for the aerodynamic design of aircraft configurations [5]. The major difficulty in using this approach is the definition of the appropriate adjoint equations for viscous flows.

In this work we explore the use of iterative methods. We have chosen two approaches: a classical gradient based cost function minimization algorithm and an evolutionary strategy (ES). Both have been successfully applied to shape optimization problems at the Center for Turbulence Research at Stanford. In the first approach, a cost function characteristic of the performance of the sail is minimized with respect to one or more control parameters. The iterative procedure requires the calculation of the derivatives of the cost function with respect to each of the control parameters in every iteration step. The second optimization approach uses evolutionary algorithms (EAs). EAs are biologically inspired optimization algorithms, imitating the process of natural evolution. EAs do not require gradient evaluations, but use a set of solutions (population) to find the optimal designs. The population-based search allows parallelization, and may avoid premature convergence to local minima. However, the population normally must be large, thus requiring many flow calculations.

Coupling optimization algorithms with CFD calculations requires the integration of various subsystems, such as the grid generation tool, the flow solver, and the optimization algorithm. Initially, we consider a simplified two-dimensional model to facilitate the development of the optimization procedure. We design the procedure so that it can be directly extended to the 3D case. In addition, it is possible that the two-dimensional model will be able to guide the three-dimensional optimization. Once both models have been implemented we will compare the 2D optimization results to the 3D results to evaluate the need for the more expensive 3D calculations.

1.1 Application and Development

Because of the complexities involved with developing a general sail shape optimization method we start with a relatively simple application that however still yields insight into the general problem. We optimize the yard-camber and sheeting angles of the rig of a modern clipper ship the *Maltese Falcon* for upwind performance in moderate winds. As shown in figure 1 three masts resembling airplane wings constructed of yards with circular arc cross-section will rig this future mega-yacht. The *Maltese Falcon* will be 87 meters length overall, have a mast height of 53 meters off the water and have a maximum yard length of 22 meters. The rig is based on an original design by W. Proells, which was further developed at Hamburg University in the early 1960's [7] and is currently being developed by designers from Gerard Dijkstra & Partners and Doyle Sailmakers. Experimental wind-tunnel data are available and eventually real-world measurements will be produced. This will allow a direct assessment of the numerical code.

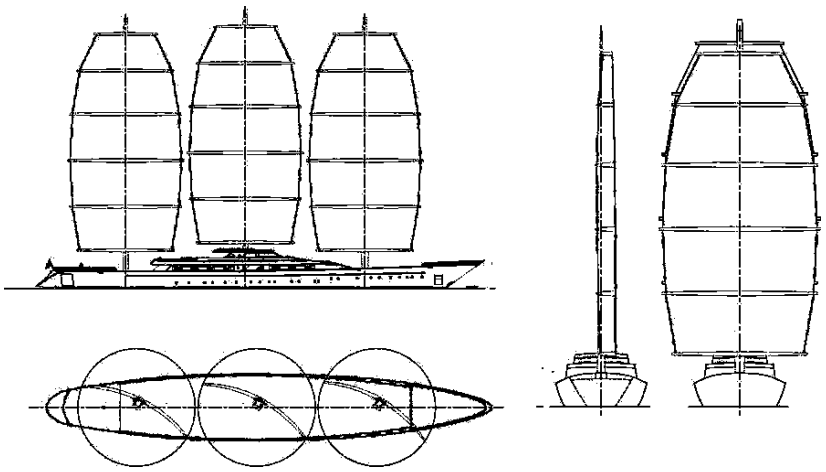

Figure 1. Initial Geometry.

From a computational modeling point of view this rig is attractive because the flying shape of the sails will be very close to the shape of the yards. This is due to the construction of the rig, which consists of yards with sails stretched between them. We therefore do not have to calculate the true flying shape of the sails, (which typically requires the coupling of the fluid model with a structural model to evaluate deformations under aerodynamics loads) Although the sails will slightly deflect in reality, it is believed that the deformation will not significantly influence the forces on the rig. In addition, the span-wise variation of the sail cross section is very limited and wind tunnel tests conducted with a model of the rig showed streamlines (visualized using smoke) that are mainly two-dimensional except near the top and bottom of the rig.

2 Evolutionary Strategies and Gradient-based Shape Optimization

The general objective is the minimization of a properly constructed cost function. The function is characteristic of the performance, and depends on a set of control variables. Two optimization algorithms are being developed both originating from algorithms that have been successfully applied in past CFD shape optimization studies at the Center For Turbulence Research.[4] One optimization method is based on a classical gradient-based optimization algorithm and the other on the concept of Evolutionary Strategies.

2.1 Gradient Based Optimization

The gradient-based optimization procedure requires the evaluation of the derivatives of the cost function with respect to the control parameters in each iteration step. A simple finite difference method is used to calculate the derivatives numerically as:

[4] The Center for Turbulence Research (CTR) is a research consortium for fundamental study of turbulent flows. It is jointly operated by Stanford University and NASA Ames Research Center.

$$\frac{dJ}{d\theta_i} \approx \frac{J_{new} - J_{old}}{\Delta\theta_i}, \quad i = 1,2,3 \qquad (1)$$

These derivatives determine the direction of improvement. On the following iteration a step is taken in this direction and the procedure is repeated until convergence [11].

$$\theta_{i,new} = \theta_{i,old} - g\frac{dJ}{d\theta_i}, \quad i = 1,2,3 \qquad (2)$$

The weighting parameter g is used to weight the gradient information and changes with cost function and control variables.

It is important to note that during each iteration the number of flow calculations needed equals $1+N$ where N is defined to be the number of control variables. Present simulations include 6 control variables and only take a few minutes to complete one iteration. But, three-dimensional simulations, or an increase in the number of control parameters, will make the current procedure computationally expensive.

In our studies, we determined an appropriate g by trial-and-error. A comprehensive sensitivity study will be performed in the future.

2.2 Optimization using Evolutionary Strategies

An evolutionary algorithm tries to mimic natural selection to determine the optimal shape. At each step random mutations (changes) to the control variables are attempted and only those solutions that are better than their predecessors are selected in a method that resembles the survival-of-the-fittest natural selection. Again a cost function representing performance is defined to compare one solution to another.
Our initial implementation is based on a very simple evolutionary strategy called a One + One ES [6]. In this implementation an initial solution J_{parent} is first calculated, then each control variable is perturbed (using a random Gaussian distribution with standard deviation S), and a new solution J_{childn} is evaluated. The new solution is compared with the old solution, and if $J_{child} < J_{parent}$ the child becomes the new parent for the next iteration. The standard deviation is adjusted using Rechenberg's *1/5* rule: every $N*L$ iterations (where N equals the number of control variables and L is a constant) increase the standard deviation if the success rate is higher than *1/5* and if not decrease the standard deviation. As the iterations proceed and the optimal solution is approached, the standard deviation continues to drop. In this work, we use L=10. Again, further analysis is necessary to determine the optimal choice.

3 Sail Shape Optimization

When applied to sail shape optimization the control variables are the parameters that define the sail configuration. In our case the relevant control parameters are the camber of the yards and the sheeting angle. Initially we will apply the optimization method to a 2D model of a horizontal cross-section of the rig (taken mid mast).

In this study we are interested in optimizing the upwind performance of the *Maltese Falcon* in moderate winds. As mentioned earlier, defining the cost function is a difficult task in upwind conditions. Ideally the cost function would be the VMG predicted with the use of a VPP, to take into account the hull/sail interaction. Presently we do not have access to hull performance data so in order to develop our procedure we consider simplified cost functions. Possible simplified cost functions are driving force, driving force to heeling force ratio, lift produced or ratio of lift to drag. Initial sheeting angle and camber optimization have been conducted and results are presented in section 4.

3.1 Simplified Two Dimensional Model

Our simplified model has nine control parameters comprised of the three sheeting angles (θi, i = 1,2,3), the three cambers (Ci, i = 1,2,3), and the three chord lengths (CHi, i = 1,2,3) as shown in figure 3. The total force on the rig can be divided into components of lift (Cl) and drag (Cd) or alternatively heeling force (Cy) and driving force (Cx). The other variables in our two-dimensional model are the apparent wind direction and velocity. Initially we consider the chords to be defined by the chord lengths approximately half way up the mast taken from the profile of the original design, but eventually the chord lengths may also be optimized. Because the chord lengths vary in the span-wise direction the spacing between sections at different heights also changes. To date the effect of the spacing (the distance between the 2D sections) has not been investigated but is believed to be an important parameter, and will be the subject of further study.

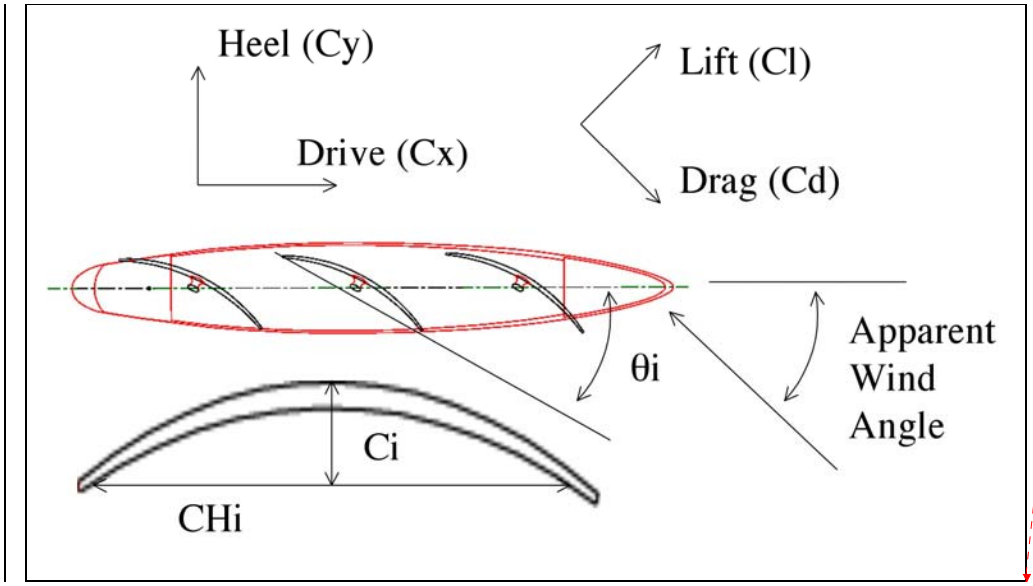

Deleted:

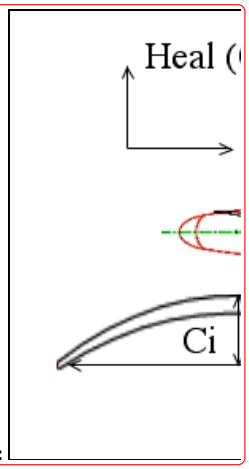

Figure 2. Simplified 2D model.

3.2 Flow Solution

The flow past the sails is calculated using FLUENT 6.0. We use Fluent's incompressible Reynolds Averaged Navier-Stokes (RANS) solver on non-conformal unstructured grids. In general, unstructured grids (as opposed to structured grids) are more flexible in terms of being able to handle complex and dynamic geometry. Because of the high Reynolds number of the sail flows (of the order of one million), turbulence modeling is required. The turbulence model used in the present calculations is the Spalart-Allmaras turbulence model, which is sufficiently accurate for upwind and close reaching conditions, and computationally efficient [1]. More sophisticated turbulence models must be used for larger angles of incidence because of flow separation. We note that in all our cases, the angles of incidence are sufficiently small to use the Spalart-Allmaras model. We investigated the realizable k-epsilon model as well, but the differences in results were too small to influence the optimization results.

In order to couple FLUENT with our optimization procedure it is necessary to automate the solution process. The automation is accomplished using FLUENT's scripting capability. A central program serves as the interface between the flow solution and the optimization algorithms. The flow solution interface takes as input the sheeting angles, cambers and chord lengths of each of the sections together with a description of where each section is placed relative to the center of each mast. A grid is automatically created from the input geometry and then the flow solution is calculated. The entire process takes around 1 minute to produce a solution on an Athlon computer with a Pentium IV 1.2 GHz processor using a relatively coarse grid of around 7500 elements. Figure 4 shows a system diagram of the automated solution procedure.

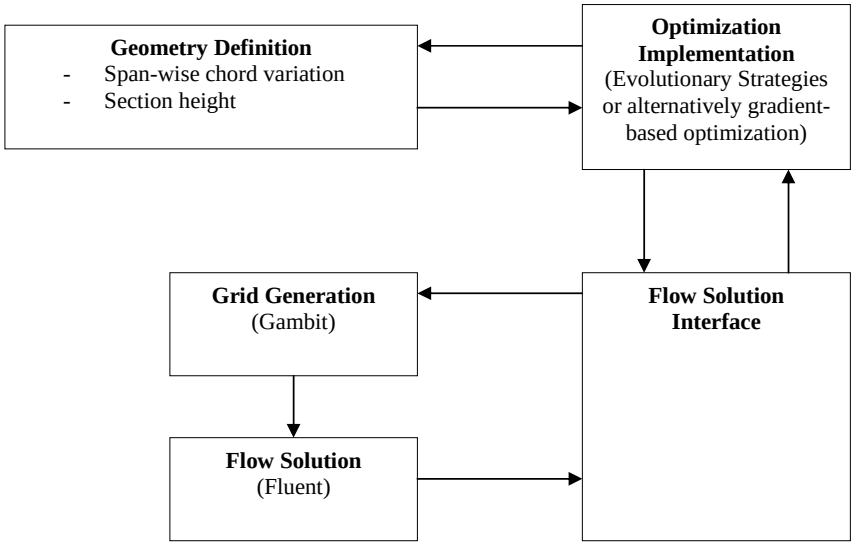

Figure 3. System diagram

3.3 Automatic Grid Generation

The most challenging aspect of automating the flow solution procedure is the robust and efficient generation of grids to discretize the domain of interest. Here, robust refers to the ability to successfully generate meshes for any possible value of the control parameters. The mesh generation is efficient if it clusters grid points in areas where large gradients of flow variables are expected (such as in the boundary layers) so that a minimal number of grid elements are required to obtain accurate predictions.

The grid generation process starts with defining the three sectional shapes. Once the sections have been defined the region immediately surrounding the sail is clustered densely with grid points in order to properly resolve the boundary layer. Because the gradients are smaller in the stream wise direction than the wall normal direction, we use quadrilateral elements with large aspect ratio. The Spallart-Allmaras turbulence model requires the distance between the first grid point away from the wall to be placed at a non-dimensional distance known as y+ on the order of 1. After meshing the region immediately adjacent to the sail the remaining domain is discretized using triangular elements. The use of non-conformal grids allows a mismatch between the grid points on the boundary of the inner and outer regions. Fluent uses interpolation to communicate the flow variables from the inner to outer regions.

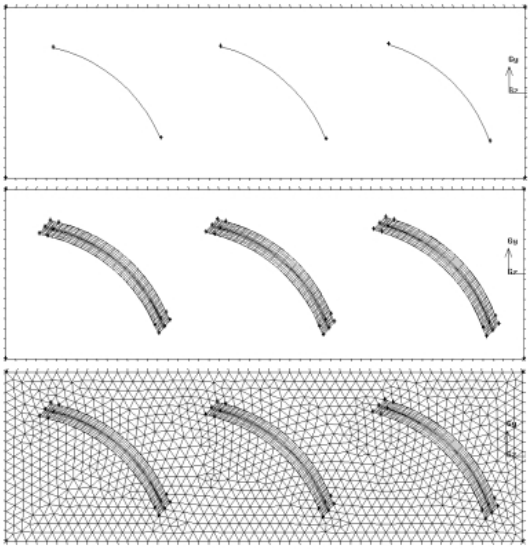

Figure 4. Automatic grid generation.

Triangular elements are used because the algorithm used by Fluent's grid generator Gambit to produce triangular elements is robust, and can handle the varying geometry created by adjusting the camber and sheeting angle of the sections. Quadrilateral elements require fewer elements to discretize the same volume but the current algorithm available in Gambit is not reliable in handling this geometry. We extended the far field region to roughly 20 chord lengths in all directions and discretized it with quadrilateral elements. The entire process is shown in figure 4.

In the three-dimensional model we intend to build the grid by first defining the cross sections at each yard and then connecting the points vertically to define the volume surrounding the sail. The masts will be included in the three-dimensional model.

4 Results

4.1 Initial Tests

Initial tests were performed on circular arc cross sections to verify our numerical solution method and to gain a better understanding of the aerodynamic properties of such foils. The first test compares values of Cl and Cd produced by 2D sections of 8,10,12 and 14 percent camber for angles of incidence in the range of 0-11 degrees. The 12 percent camber section is seen to have the highest lift/drag ratio. For all the sections the maximum lift/drag ratio is achieved at the correct angle of incidence.

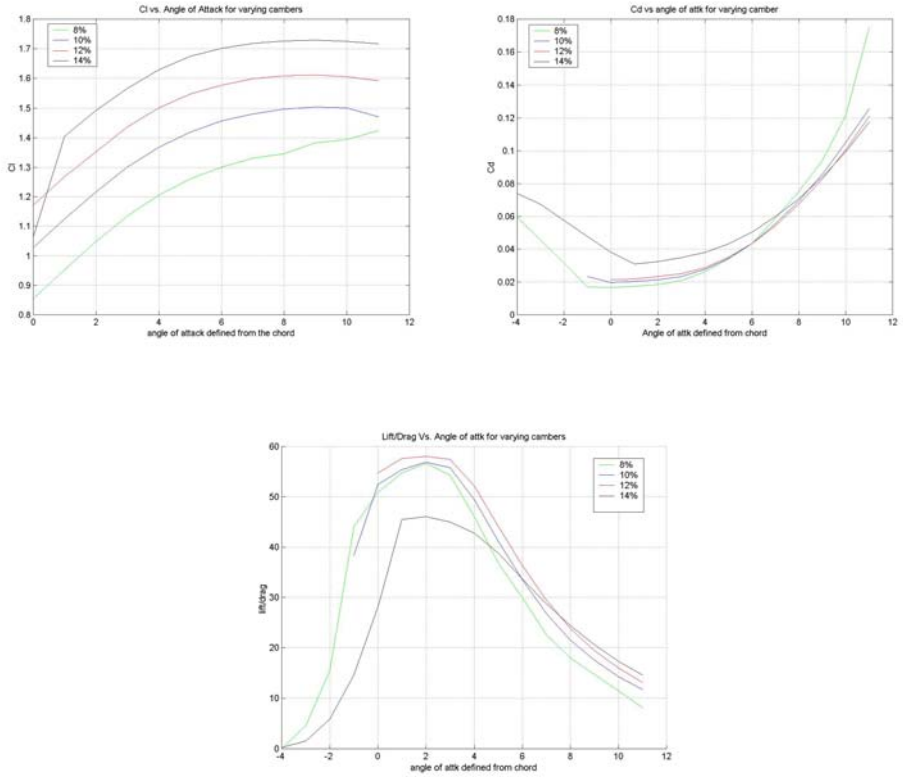

Figure 5. Plots of Cl,Cd and Cl/Cd for circular arc sections of various camber.

The forces presented in Figure 5 are plotted as functions of the angle of incidence defined from the chord. As mentioned previously, one of the challenging aspects of sail shape design is that as the sheeting angle (or apparent wind angle) changes, the contributions of the lift and drag forces to the driving force and heeling force change. Figure 6 shows the driving force (Cx) and heeling force (Cy) as functions of the apparent wind angle.

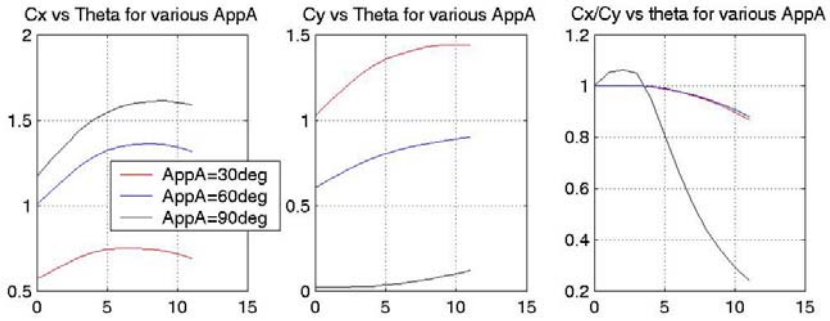

Figure 6. Projection of Cd and Cl onto Cx and Cy for various apparent wind angles.

We note that we have performed several tests to validate the flow results, including grid convergence studies, and comparisons between various turbulence models and gridding strategies. We are confident that the methods and models we use are sufficiently accurate for our purposes.

4.2 Sheeting Angle Optimization

The first step in developing an automated sail shape optimization procedure is to ensure that for a given apparent wind angle the sails are set in the optimal configuration. This is straightforward for a single section. Once lift and drag are determined as functions of the angle of attack, the sheeting angle can be set to produce the angle of incidence that optimizes the performance for the given apparent wind direction. With three interacting sections, however, the flow field is dependent on all three sheeting angles and there is no easy way to predict the optimal sheeting angles.

Initially, we consider two simple cost functions *J1* (max Cx) and *J2* (max Cx/Cy). Optimization runs are performed for both cost functions for apparent wind angles ranging from 30 to 90 degrees. Both optimization strategies were used and lead to identical results with comparable runtimes.
We present results for apparent wind angles of 30, 60 and 80 degrees in table 1 and figure 7. Table 1 displays the driving force and heeling force coefficients for each apparent wind angle for both cost functions. The optimal sheeting angles are also given. Figures 7 shows plots of static pressure around the sail as well as the pressure distribution on each section.

30 degrees apparent wind angle					
Cost function	*Force coefficient*		*Sheeting angle*		
	Driving	*Heeling*	*Aft*	*Mid*	*Fore*
J_1	0.9304	1.9038	-6.5	-19.3	-31.6
J_2	0.7988	1.4754	-16.0	-26.6	-36.1
60 degrees apparent wind angle					
J_1	1.4943	1.0116	-42.6	-49.9	-55.8
J_2	1.1327	0.6888	-56.0	-57.3	-60.9
80 degrees apparent wind angle					
J_1	1.6193	0.3893	-68.45	-70.90	-73.12
J_2	1.2571	0.2499	-77.17	-78.34	-79.60

Table 1. Force coefficients and sheeting angles for optimal sail configurations.

For all apparent wind angles tested, cost function J_2 results in more open (larger angle) sheeting

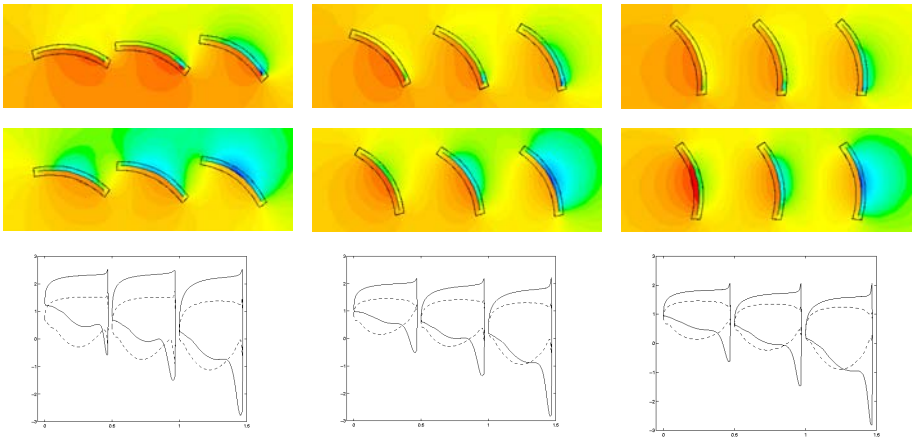

Figure 7. Top: Static pressure contour plots corresponding to *J1* ; Mid: Static pressure contour plot corresponding to *J2* Bottom: Pressure distribution along the sail chord.

arrangements with a more even pressure coefficient distribution along the length of the sail cross sections. It is interesting to note that if telltales are imagined to be placed on the leading edge of the sails as shown in figure 8, cost function *J1* results in an over-trimmed sail with the leeward telltale lifting, while cost function *J2* results in a well trimmed sail with both telltales streaming back.

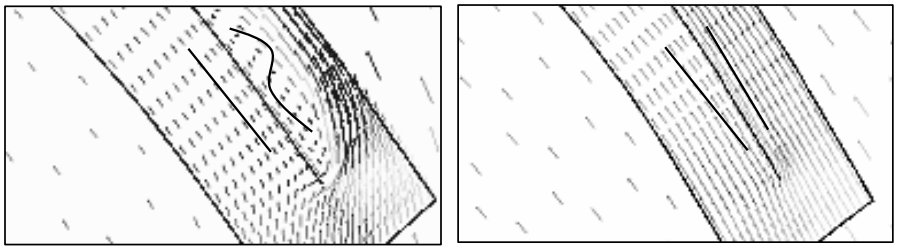

Figure 8. Telltales imagined to be on the leading edge of the sail are shown to lift for *J1* indicating an over-trimmed sail and stream back for *J2* indicating a properly trimmed sail.

4.3 Sheeting angle and Camber Optimization

Initial camber optimization runs have been performed to investigate the influence of section camber on rig performance. All runs started with 12 percent camber sections and the optimal sheeting angles presented in sections 4.2. In these runs, we maximized the sheeting angles at the same time as the section camber. A summary of the results is presented in table 2. Results are presented only for maximizing the driving force as problems with convergence prevented conclusive results for optimizing the driving force to heeling force ratio. A problem with the evaluation of the gradient with respect to the camber is believed to be preventing convergence.

30 degrees apparent wind angle									
Cost function	*Force coefficient*		*Sheeting angle*			*Camber % of chord*			*% J1 increase over 12% camber*
	Driving	*Heeling*	*Aft*	*Mid*	*Fore*	*Aft*	*Mid*	*Fore*	
J_1	1.14	2.35	-0.5	-15.3	-33.5	14.2	16.8	22.8	18
60 degrees apparent wind angle									
J_1	1.96	1.29	-42.0	-48.6	-58.8	19.4	18.7	26.8	23
80 degrees apparent wind angle									
J_1	2.39	0.57	-68.2	-71.9	-75.5	30.9	24.4	21.0	32

Table 2. Force coefficients, sheeting angles and camber for optimal sail configurations

Streamlines are shown in figure 9 for the optimal configurations calculated for maximum driving force. The cambers selected to optimize the driving force are seen to be greater than the original 12% sections in all cases. For apparent wind angles of 60 degrees and 80 degrees maximizing the driving force can be considered a reasonable cost function but for an apparent wind angle of 30 degrees the heeling force needs to be accounted for. The results for maximizing driving force at 30 degrees are presented as reference to compare with the results found in the previous subsection for optimizing the driving force at 30 degrees with only the sheeting angles as control parameters. It is interesting that the optimal sheeting angles found here are not much different from the initial angles chosen, even though the optimized cambers are.

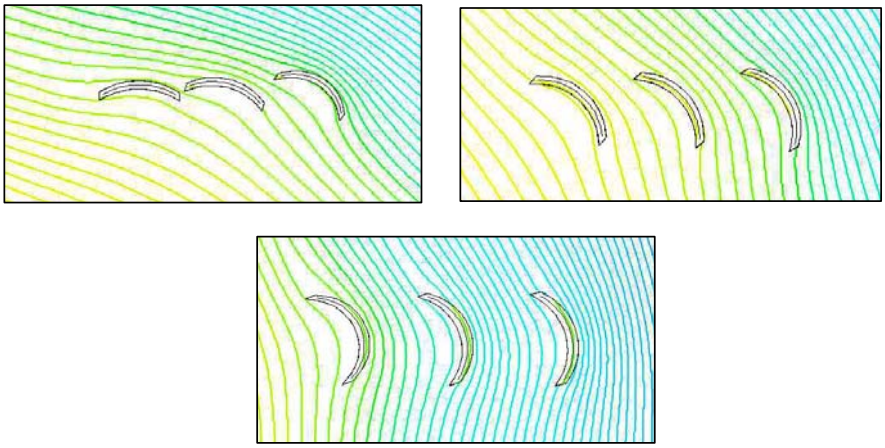

Figure 9. Streamlines for maximum driving force for apparent wind angles of 30 deg (top left), 60 deg (top right) and 80 deg (bottom).

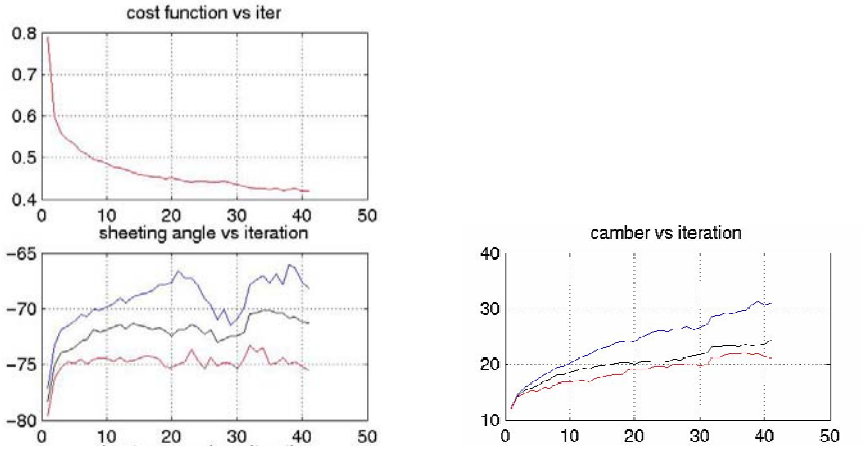

Figure 10. An example of the optimization procedure is reported; for each iteration the cost function and the parameters (cambers and sheeting angles) are represented. The optimization is considered complete when the cost function reaches a plateau.

Formatted

Deleted:

5 Discussion and Future Work

A CFD-based optimization procedure for sail configuration has been developed and applied to two-dimensional sections of a three-mast clipper ship, the *Maltese Falcon*.

Optimization runs were conducted using both the gradient-based optimization method and the method based on evolutionary strategies. Both methods converge to the same solution in about the same amount of time. Both algorithms should be investigated further to try to optimize their performance.

The major burden in the gradient-based methods is the calculation of the derivative of the cost functions with respect to the parameters. It is likely not necessary to compute the gradients exactly and we will explore the use of cheaper approximations.

The value of the parameter g greatly influences the convergence rate of the gradient-based algorithm. The value we used in this work was found by trial-and-error. A more thorough sensitivity analysis is required. Within the One + One ES the selection of the initial standard deviation and the constant *L* should be investigated. In addition, the One + One ES is the simplest possible ES and there are other strategies that use larger sets of populations to arrive at the optimal configuration.

In this paper we presented the design of our optimization method, and the development of the basic optimization tools. We are currently working on:

- Further validation of the various components of the two-dimensional optimization strategy
- Development of a more realistic performance evaluation model that takes both hull and sail forces
- Refinement of our optimization goals to more accurately reflect the optimal aerodynamic characteristics of the rig.

A more realistic model of the actual performance of the rig necessitates the development of a three-dimensional optimization strategy. Once the three-dimensional model has been implemented, 2D and 3D results will be compared. . In contrast to 3D flow simulations, 2D simulations cannot compute the induced drag of the sails, which is a large component of total drag in upwind conditions. We are interested in assessing how much induced drag influences the optimization results. We plan to develop a procedure for estimating the induced drag based on two-dimensional sail flow simulations. Similar strategies have been successfully applied to airfoil simulations for many years. We will also investigate the validity of the steady state assumption we make. We want to determine whether optimizations conducted in steady state can accurately optimize the actual dynamic performance of the ship, and if not how to best take into account unsteadiness.

To develop more realistic optimization criteria we plan to work directly with the Maltese Falcon designers to gain a better understanding of what is needed from the rig to produce optimal performance. We will determine if integration with a VPP is necessary, or if smart and simple modifications to the cost functions can be made to take into account the interaction with the hull forces.

- **References**

1. Collie, S., Gerritsen, M. & Jackson, P. (2001), "A Review of Turbulence Modelling for Use in Sail Flow Analysis", *School of Engineering Report No. 603*, University of Auckland, New Zealand.
2. Kim, S., Alonso, J. & Jameson, A. (2002), "Design optimization of High-Lift Configurations Using a Viscous Continuous Adjoint Method", *AIAA Paper 2002-0844*, 40th Aerospace Sciences Meeting and Exhibit, Reno, NV, January 2002.
3. Marchaj, C.A., (2000) Aero-hydrodynamics of Sailing, 3rd edition, Adlard Coles Nautical, London.
4. Mohammai, B. & Pironneau, O. (2001), *Applied Shape Optimization For Fluids*, Oxford University Press.
5. Reuther, J., Jameson, A., Farmer, J., Martinelli, L. & Saunders, D. (1996), "Aerodynamic Shape Optimization of Complex Aircraft Configurations via an Adjoint Formulation", *AIAA Paper 96-0094*, 34th Aerospace Sciences Meeting and Exhibit, Reno, NV, January 1996.
6. Sbalzarini, I., Su, L. & Koumoutsakosyz, P. (2000) "Evolutionary optimization for flow experiments", *Annual Research Briefs 2000*, Center for Turbulence Research, NASA Ames/Stanford Univ., 31-43.
7. Wagner, B. (1976), "Sailing Ship Research at the Hamburg University. A survey of the activities in the years 1961-1967", *Symposium on the Technical and Economical Feasibility of Commercial Sailing Ships*, Liverpool Polytechnic Department of Maritime Studies, February 1976.